EFFECT OF WOLLASTONITE AND COLLOIDAL NANO-SILICA ON MECHANICAL, AND DURABILITY PROPERTIES OF CEMENT MORTAR

NISHANT A NAIR, VISWANATHAN T S*
School of Civil Engineering, Vellore Institute of Technology, Vellore-632 014, Tamil Nadu, India

This article aims to produce sustainable and durable mortar with help of wollastonite admixing with Pozzolan portland cement with and without nano-silica. Wollastonite was chosen for its flexural capacity and nano-silica for refining the pore matrix and improving the overall properties of the mortar matrix. At 3, 7, and 28 days, eight different mix proportions were investigated. The ease with which water moves through the mortar medium and also porosity parameters were used as durability indicators. Mechanical properties tested were compressive strength, flexural strength, and dynamic modulus of elasticity. Correlations of mechanical properties were found using a graphical method. X-Ray Diffraction (XRD) and Fourier Transform infra-red (FT-IR) spectroscopy were employed to characterize the samples taken from the fractured specimens. Pore radius was calculated with the help of sorptivity and permeable porosity values. In terms of mechanical and durability properties, wollastonite replacement at 10% and nano-silica replacement at 6% were found to be optimum.

Keywords: Wollastonite, nano-silica, sorptivity, porosity, pore radius

1. Introduction

Greenhouse gas emissions can be reduced in the construction industry by reducing cement consumption or using carbon capture and sequestration (V. Dey et al. 2015; Deng et al. 2013; Svensson et al. 2018). Carbon capture and storage are not without their own set of constraints. The most straightforward option is to reduce the consumption of cement.

Wollastonite is a white-colored natural mineral with an acicular structure that can be used for partial substitution of cement. The particles of this material are fibrous due to their acicular structure (Kwon et al. 2015; V. Dey et al. 2015; Deng et al. 2013; Soliman and Nehdi 2012). The fibrous structure of wollastonite can help the cement-wollastonite matrix improve the flexural property. The stoichiometric formula for wollastonite is $CaSiO_3$. Wollastonite is also classified as a Class C pozzolan based on its primary composition (Ransinchung and Kumar 2010; Nair and Sairam 2021). Compressive, and flexural strength, water absorption properties, and chloride ion penetration of paving concrete (Mathur et al. 2007) and cement-silica fume concrete (Ransinchung, Kumar, and Kumar 2009) were studied. The study on wollastonite-recycled waste ceramic aggregates and micro-silica effects on the durability of high strength concrete (Zareei et al. 2019). The ductility of wollastonite microfibres was studied in an ultra-high-performance mortar (Kwon et al. 2015).

Nano-silica's addition increases the mechanical and durability properties of concrete and mortars nano-silica is used to spread the nanoparticles more evenly and because dry silica (Naji Givi et al. 2010; U. Sharma et al. 2019; Li and Ding 2003). Nano-silica has a very high specific surface area which facilitates very high reactivity and accelerates hydration (Aggarwal, Singh, and Aggarwal 2015; Qing et al. 2007). Nano-silica increases the pore size distribution and densifies the paste, which improves the mechanical and durability properties of the paste even at an early stage (Zhang, Islam, and Peethamparan 2012; U. Sharma et al. 2019). Colloidal nano-silica accelerates the formation of gel structure and hydration at an early age (Hou et al. 2013).

Sorptivity is a long-proven measure for concrete durability based on water movement through unsaturated materials like stone, brick, and construction material (Christopher Hall and Hamilton 2018; C. Hall 1989; Christopher Hall and Hoff, n.d.). Many parameters such as pore radius, capillary moisture content, and nonlinear hydraulic diffusivity can be mathematically derived from sorptivity (Feng and Janssen 2018; Christopher Hall and Hoff, n.d.; Hanumanthu and Sarkar 2021). Sorptivity depends on functions like density, surface tension, pore radius, capillary continuity, tortuosity, and surface tension of a liquid (Uzoegbo 2019).

The objective of this study is to find the optimum dosages of wollastonite and nano-silica with help of mechanical, durability, and microstructural studies focusing on porosity of the mortar matrix. There is little or no information about sorptivity and water absorption studies conducted on mortars containing wollastonite and nano-silica. From these durability studies porosity can be studied. Colloidal Fig. 1 - Wolkem India limited provided the wollastonite Kemolit H3 (N). Colloidal nano-silica cembinder 8 was provided by Nouryon Company. Sand utilized as per ASTM C33. The water/binder ratio was kept at 0.50

*Autor corespondent/*Corresponding author*,
E-mail: viswanathan.ts@vit.ac.in

cannot utilize the entire specific surface area of particles, therefore colloidal nano-silica was used. Nanosilica also refines the pore structure. The nano-silica dosage is limited to 6% from an economic point of view. From porosity and sorptivity values, the pore radius is calculated (Yang et al. 2019). These parameters are correlated with mechanical properties such as compressive strength, flexural strength, and dynamic modulus of elasticity using the graphical method.

2.Materials and methods

Pozzolana Portland cement (PPC) conforming to type IP according to ASTM C595 was used.

for the control mix and other mixes. The mortar was mechanically mixed as per ASTM C305. The binder to sand ratio was maintained at 1:2.75. Table 1 shows the mix designation used in this paper. Fig. 1 shows the Field emission scanning electron microscope (FESEM) image of wollastonite H3 having a fibrous structure.

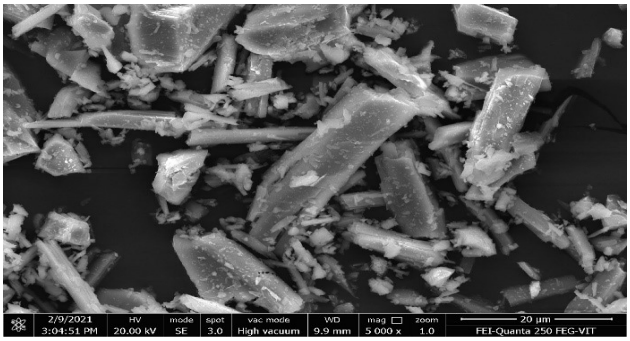

Fig. 1 FESEM image of wollastonite

Table 1. Mix designation descriptions

Sl. No.	Mix Designation	Cement (% of total binder)	Wollastonite (% of total binder)	Nano-silica (% of total binder)
1	C0	100	-	-
2	H10	90	10	-
3	H20	80	20	-
4	H30	70	30	-
5	NS 1.5	88.5	10	1.5
6	NS 3	87	10	3
7	NS 4.5	85.5	10	4.5
8	NS 6	84	10	6

Wollastonite and nano-silica physical properties are shown in table 2 (a & b).

Table 2ª. Wollastonite Physical properties (Kwon et al. 2015; Bian et al. 2016; Mathur et al. 2007)

Material	Density,g/cc	Specific gravity	Mohr's hardness	Bulk density, g/cc
Wollastonite	2.8	2.9	5	0.6

Table 2b.
Nano-silica Physical Properties (Levasil, n.d.)

Material	SiO_2 content	Density, g/cc	pH	Viscosity, cP
Colloidal Nano-silica	50 % by wt	1.4	9.5	8

Sorptivity test and density, absorption, and voids test has been conducted under ASTM C1585 and ASTM C642 respectively under durability parameters. The specimen conditioning is done to achieve a moisture content of 40-60% to experiment with specimens exposed to natural climate *(DeSouza, Hooton, and Bickley 1997)*.

2.1 Material Characterization

The samples were collected from specimens after the compression test and sieved in a 90-micron sieve. The collected sample was then dipped in isopropyl alcohol to arrest hydration (Kondraivendhan and Bhattacharjee 2010).

XRD is one of the most renowned characterization techniques currently available for fine-grained crystalline materials. XRD was carried out by powder X-ray diffractometer-Bruker, D8 *advance.* Here, quantitative phase analysis (QPA) of the sample is carried out. QPA is the comparison of obtained XRD patterns with an already existing database of phases (scrivener, Snellings, and Lothenbach 2016).

FESEM is an imaging technique that gives the morphology of a given material (scrivener, Snellings, and Lothenbach 2016). FESEM analysis was conducted in Thermo Fisher FEI-Quanta 250 FEG having an operating voltage between 5kV-30kV, and a resolution of 1.2 nm in vacuum conditions.

FT-IR spectroscopy determines the functional group of molecules, as such groups have fundamental vibrations based on irradiation from different wavelengths of light. FTIR was conducted by Shimadzu IRAffinity-1 mid IR range equipment (4000-400 cm^{-1}) with 0.5-16 cm^{-1} resolution.

2.2 Mechanical properties

Compressive strength was analyzed as per ASTM C109 using 50 mm mortar specimens. A flexural strength test was conducted on an electromechanical Universal testing machine (EUTM). The rate of displacement of the machine was fixed at 0.1 mm/sec (Soliman and Nehdi 2012). Flexure test was conducted after 7 and 28 days of curing.

An ultrasonic pulse velocity (UPV) test was conducted to determine the DYM by IS: 13311-2004. Fig. 2 shows the ultrasonic pulse velocity equipment.

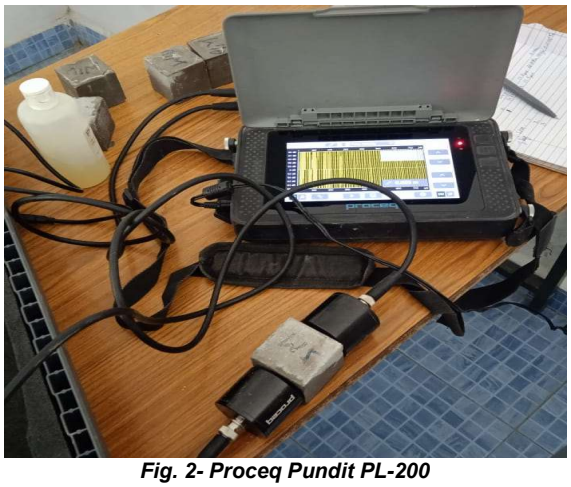

Fig. 2- Proceq Pundit PL-200

2.3.Durability properties

Water absorption test was conducted in accordance with ASTM C642. Water absorption was conducted on 3 specimens for each mix proportion/ curing age. Sorptivity was conducted as per ASTM C1585, and 2 numbers of cylindrical specimens for each mix/curing age was experimented.

3.Results and discussions

3.1 Compressive strength

The compressive strength values of all the mixes at different curing ages have been presented in table 3. Compressive strength decreased with decreasing cement content except for 10% wollastonite replacement. Amongst the wollastonite-only mixes, H10 showed better compressive values than the control mix, hence it was selected as optimum. Nano-silica was added to H10 mixes as cement replacements. The lowering of compressive strength as wollastonite content increases can be attributed to the dilution effect. The strength improvement at later stages of curing is due to improvement in matrix-microfibre bond (Soliman and Nehdi 2012) and pozzolanic activity of wollastonite (Ransinchung and Kumar 2010). The compressive strength increases with a dosage of nano-silica compared to the control mix. NS6 was 33% and 34% higher and H30 was 8.7% and 10% lower compared to the control mix at 7 and 28 days, respectively. The increase in compressive strength due to partial replacement with nano-silica can be attributed to void filling in early-stage mortar matrix hydration, and as an activator to fasten the pozzolanic reaction due to very high specific surface area resulting in the formation of additional CSH gel (U. Sharma et al. 2019; Levasil, n.d.).

3.2 Flexural strength

Flexural strength was investigated to ascertain the bond strength between wollastonite microfibres, nano-silica, and cement matrices. Due to the fibrous nature of wollastonite, H30 showed the highest flexure strength among wollastonite mixes. At 7 and 28 days, H30 achieved 19% and 10% flexural strength higher than the control mix, and NS6 flexural strength was 35% and 14% more than the control mix, respectively. The load vs displacement graph for the mixes containing wollastonite showed failure at very high displacements. Wollastonite helped delay the onset of the first crack by bridging the micro-cracks (Soliman and Nehdi 2012). The mechanism by which nano-silica enhanced the flexural strength can be attributed to the matrix being densified by homogeneously placed nanoparticles(Naji Givi et al. 2010; Jo, Kim, and Lim 2007). Table 3 shows the variation of flexural strength of different mixes at 7 and 28 days.

3.3 Dynamic Young's Modulus of elasticity (DYM)

H10 displayed the highest DYM amongst wollastonite mixes and 18% higher than to control mix. There is an increase in DYM compared to the control mix as the wollastonite fibers create a bridging effect through micro-cracks (Vikram Dey et al. 2016). An increase in wollastonite content facilitates increasing the porosity and thereby decreasing the DYM (J 2000). When Nano-silica was used, the highest DYM was observed in NS 6, 23% higher than the control mix as represented in table 3. The cement matrix was densified with the use of nano-silica as it reduced the porosity (Ghosh, Sairam, and Bhattacharjee 2013; S. K. Sharma 2019; Naji Givi et al. 2010).

Table 3. Mechanical properties of mortar

Mix Designation	Compressive strength, MPa			Flexural strength, MPa		Dynamic Youngs modulus, GPa
	3 days	7 days	28 days	7 days	28 days	28 days
C0	8.0	21.4	35.7	2.76	4.2	2.55
H10	10.9	24.9	39.3	2.89	4.4	2.75
H20	8.80	21.0	34.8	3.10	4.3	2.60

H30	*7.47*	*19.6*	*32.1*	*3.30*	*4.3*	*2.50*
NS1.5	*10.8*	*22.8*	*42.9*	*3.50*	*4.5*	*2.82*
NS3	*11.4*	*24.5*	*43.6*	*3.70*	*4.6*	*2.85*
NS4.5	*16.9*	*24.9*	*45.2*	*3.73*	*4.6*	*2.87*
NS6	*17.0*	*28.5*	*48.0*	*3.73*	*4.73*	*2.93*

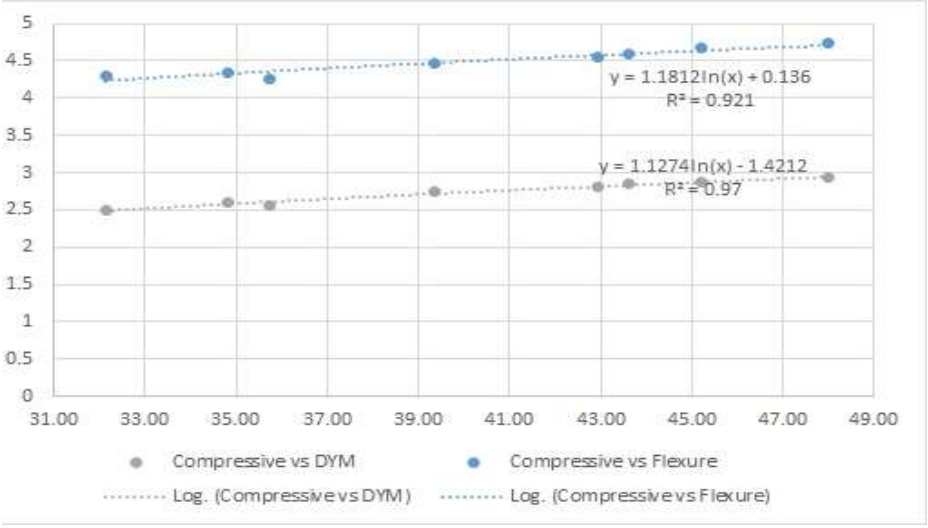

Fig. 3 - Correlation between mechanical properties of mortar

3.4 Correlation between compressive strength with flexural strength and dynamic young's modulus

The 28 days logarithmic relation between compressive strength and flexural strength with an R^2 value of 0.97 is represented in fig. 3. The relation between compressive strength and flexural strength is given in logarithmic equation 1.

$$y = 1.1812 \ln x + 0.136 \quad [1]$$

Compressive strength and DYM can be correlated by the following equation,

$$y = 1.1274 \ln x - 1.4212 \quad [2]$$

The R^2 value of both the above equations shows an excellent correlation between compressive strength, flexural strength, and DYM. The mechanical value data sets are close to the regression line.

3.5 Water absorption test

Water absorption after immersion (WAI), and water absorption after boiling (WAB) are represented in fig. 4a and 4b, respectively. In mixes containing only wollastonite, the WAI of H10, W20, and W30 was found to be 6.9%, 6.8%, and 1.8% lower than the control mix, respectively at 28 days. WAB of H10, H20, and H30 was found to be -3.9%, -4.9%, and 11% respectively compared to the control mix at 28 days. While considering the nano-silica mixes, the water absorption is further reduced due to pore refinement. NS1.5, NS3, NS4.5, and NS6 have WAI of 9.92%, 21.3%, 21.4%, and 21.9%, respectively lower than the control mix at 28 days. WAB of NS1.5, NS3, NS4.5, and NS6 at 28 days lower than the control mix are 1.74%, 4.41%, 6.71%, and 20.6%, respectively. Bulk and apparent density are represented in fig. 4c and 4d respectively. The trend shows an increase in both densities with the addition of nano-silica. NS6 has the highest bulk density which is 11.2% and an apparent density of 10% more than the control mix at 28 days. The highest bulk and apparent density among wollastonite only mix at 28 days was found in H10, i.e. 2.93% and 0.52% higher than the control mix, respectively.

Permeable voids of all mixes are given in fig. 4e. At 28 days, NS6 has the lowest pore space of 11.73% less than the control mix and H10 has the lowest pore space among wollastonite-only mixes of 1.56% to the control mix. At 3 and 7 days, a similar trend was noticed, NS6 was lowest with 16.32% and 15.35%; H10 had 0.94% and 1.77%, respectively compared to the control mix.

The absorption, density, and porosity are correlated. These parameters can also be correlated to compressive strength and DYM. NS6 shows the highest compressive strength, bulk density, apparent density, and DYM among all mixes and also has low permeable pre-space and water absorption. The mechanisms responsible for these changes are (a) pore size refinement and densification of matrix, (b) reduction of calcium hydroxide, and (c) improvement in interfacial zones of binder-aggregate (Rao 2003; Ransinchung and Kumar 2010).

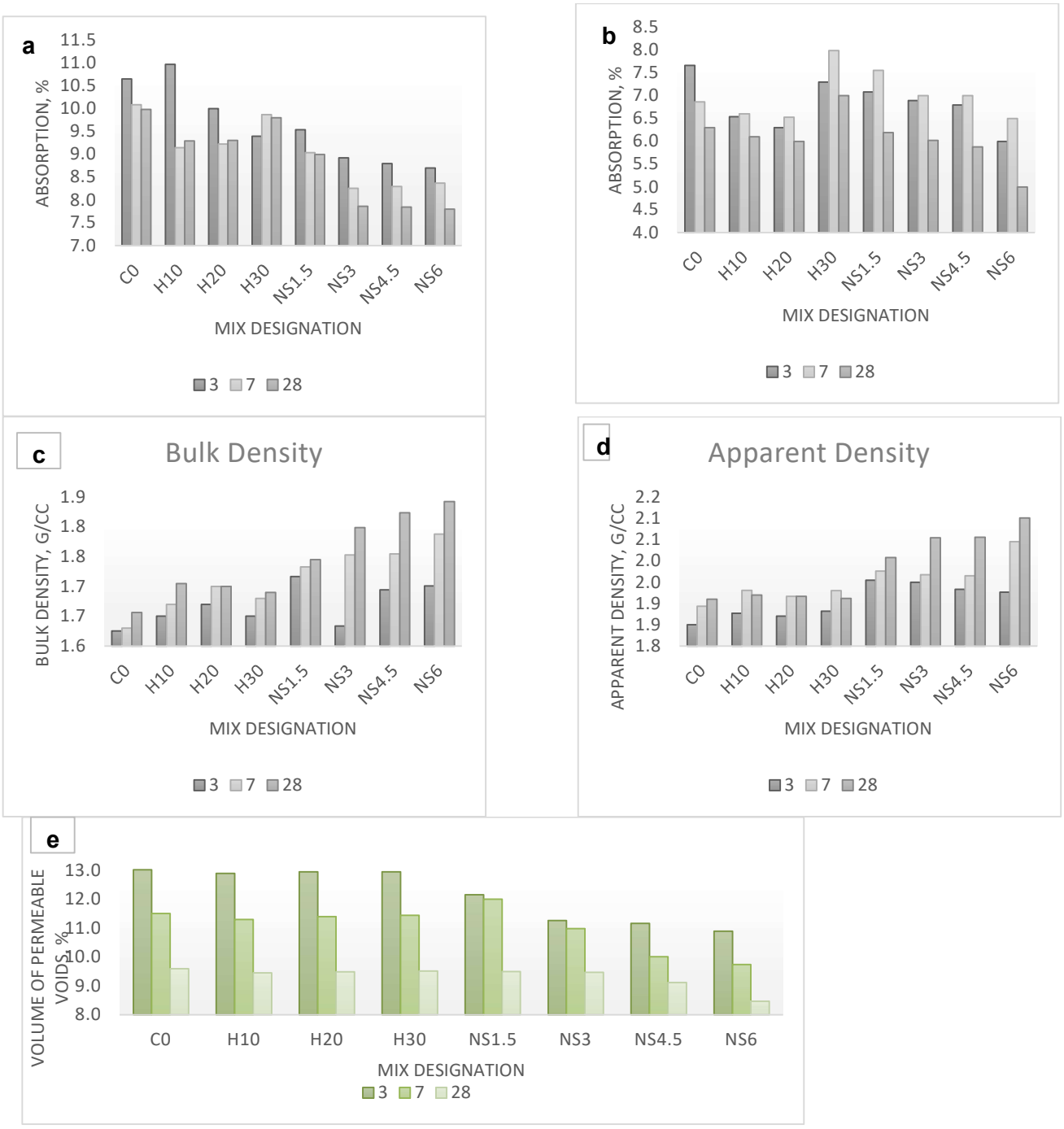

Fig. 4 - a) Absorption after immersion; b) Absorption after boiling; c) Bulk Density; d) Apparent Density; and e) Volume of permeable voids

3.6 Sorptivity

From fig. 7, we can observe that the initial rate reduces drastically as the amount of nano-silica is increased and also, there was an increase in the initial sorptivity rate as the amount of wollastonite increased. The sorptivity represents the porosity present in the mortar mixes. The least initial sorptivity was observed in NS6 at 3, 7, and 28 days at 68.8%, 69.9%, and 69.7% lower than the control, mix, respectively. Among the wollastonite-only mixes, H10 shows high initial sorptivity in 3 days but it reduces at 7, and 28 days about 26.53% and 18.33% lower than the control mix, respectively.

The secondary sorptivity and trend lines are shown in Fig. 8 for various mix designations.

In comparison to the control mix, NS6 had th e lowest secondary sorptivity at 3, and 28 days, wit h 3.3%,57.1 %, and 93.56%, respectively.

The density of the matrix and the interconne ctivity of the voids are represented by the initial an d secondary sorptivity. The fig. 7 and 8 suggest that the increase in wollastonite content of more than 10% increases the porosity of the matrix, and nano-silica reduces the water ingress to the matrix by filling the pores by forming CSH nanocrystals *(Monteiro et al. 2009)* and discontinuing the pore network.

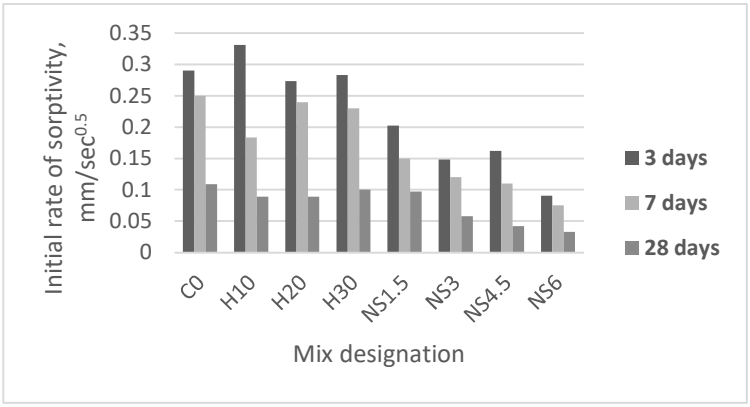

Fig. 7- Initial sorptivity

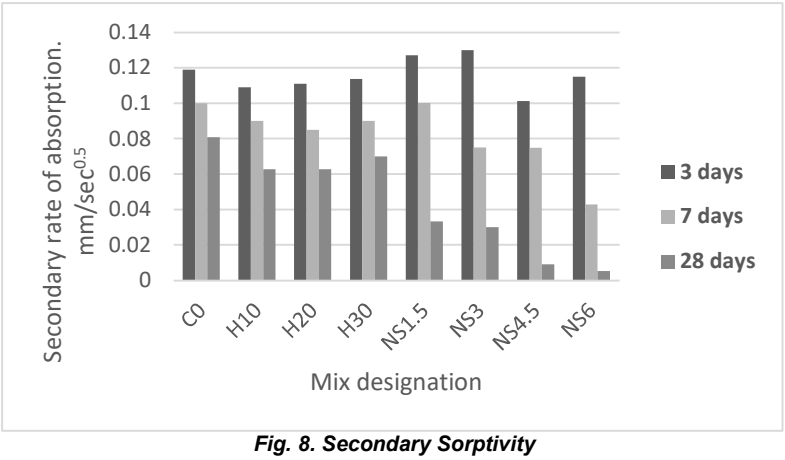

Fig. 8. Secondary Sorptivity

3.7 Pore radius

Permeable pore radius can be calculated theoretically using Hagen-Poiseuille equating and the Lucas-Washburn model *(Yang et al. 2019)*. Hagen-Poiseuille equation is given as,

$$\frac{dV}{dt} = \frac{\pi R^4 \delta P}{8\gamma H} \quad [3]$$

Where, dV/dt-Volumetric rate change, R-radius of conduit, ΔP- change in pressure, γ-dynamic viscosity of the fluid, H- depth of ingress.

Finally, the relationship between sorptivity, porosity, and pore radius is as follows:

$$R = \frac{1}{k}\left(\frac{I}{\varphi}\right)^2 \quad [4]$$

Where, R-permeable pore radius, k-constant = (γcosϴ/2η), γ-surface tension of the liquid. ϴ-contact angle of liquid, η- dynamic viscosity of the liquid, φ- porosity, I-sorptivity

The pore radius is given in table 4, we can observe that with an increase in nano-silica percentage the pore radius can be seen reducing suggesting densification of matrix and discontinuity in porosity. The discontinuity of pores can be attributed to wollastonite bridging the micro-cracks and the formation of CSH gel and nano-silica acting as fillers of pores.

Table 4
Theoretical Permeable Pore radius

Mix designation	Pore radius (m)		
	3 days	7 days	28 days
C0	1.21234E-05	5.40724E-06	1.06446E-06
H10	1.6088E-05	6.44892E-06	2.10621E-06
H20	1.12467E-05	1.13522E-05	2.19679E-06
H30	1.23475E-05	1.06895E-05	2.68091E-06
NS1.5	6.78277E-06	3.81467E-06	2.55961E-06
NS3	4.23326E-06	2.91724E-06	9.04552E-07
NS4.5	5.13711E-06	2.9532E-06	5.15979E-07
NS6	1.68241E-06	1.44916E-06	3.70887E-07

3.8 XRD

The peaks of various blends acquired by XRD are shown in Figure 9. The components of the mix are represented by these peaks and are analyzed by the Rietveld method. The creation of Calcium-Silicate-Hydrate (CSH) gel, alite (C_3S), and belite (C_2S) bogue compounds, which are crucial in the hydration process, can be seen in the XRD data. As the nano-silica with wollastonite percentage is increased, the peaks of Calcium hydroxide reduce significantly as the Calcium hydroxide is converted to CSH by nano-silica (Levasil, n.d.). The strong peaks of unhydrated compounds like alite and belite are maintained. Even the CSH gel formation shows stronger peaks with the addition of wollastonite and nano-silica. With the inclusion of wollastonite and nano-silica, the Calcium-Silicate-Hydrate gel formation also shows stronger peaks. Ettringite can be seen in peaks near 10-12 degrees.

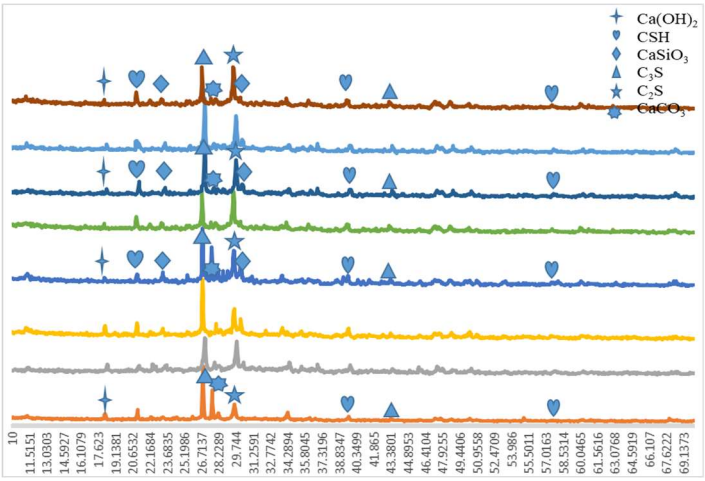

Fig. 9. X-Ray Diffraction data

3.9 FT-IR spectroscopy

Different functional groups and phases were found after 28 days of curing in various mixes by FT-IR spectroscopy. Large vibrations near 1400 cm^{-1} were observed in all mixes except the control mix. This indicates the presence of monocarboaluminate of calcium (C3A) which forms due to a reaction between CO_2 and excess calcium aluminium hydrate. Low vibrations near 3200-3400 cm^{-1} indicate the presence of hexagonal hydrates i.e. CSH gel. 420-440 cm^{-1} vibrations are associated with ettringite due to wollastonite, a natural pozzolan. The formation of monocarboaluminates hinders the conversion of ettringite to monosulphates due to the consumption of CO_2 (Scrivener and Capmas 2004; Trezza and Lavat 2001).

4.Conclusion

Admixing nano-silica with 10% wollastonite had a very positive impact on the 7 and 28-day compressive strength of mortar. The addition of wollastonite and nano-silica delayed the onset of the first crack by fusion of microcracks. DYM decreased with an increase in wollastonite microfibres due to an increase in porosity. DYM of nano-silica mixes increased due to the densification of the matrix. Water absorption and permeable pores gave corresponding values, proving that DYM reduction is due to porosity. The pore radius of nano-silica admixed mixes show lower values than the control mix. The increase in compressive and flexural strength can be attributed to the dense matrix due to the conversion of calcium hydroxide to CSH nanocrystals which also reduces the pore radius. The XRD data shows a significant reduction in calcium hydroxide when nano-silica is used. FTIR corroborates with XRD on the formation of CSH gel.

5. Acknowledgements

We sincerely thank Wolkem India Ltd for providing us with Wollastonite. We also thank Nouryon India Ltd for providing us with nano-silica (Cembinder 8). We are also thankful to VIT Chancellor, Registrar, and other VIT Higher administration group personnel who have made it possible for us to work as much as possible during this pandemic period safely and comfortably. We also would like to acknowledge the Dean, HoDs, faculties, and research scholars of the Civil Department whose inputs were taken for testing and completion of this paper.

REFERENCES

[1] Aggarwal, Paratibha, Rahul Pratap Singh, and Yogesh Aggarwal. 2015. "Use of Nano-Silica in Cement Based Materials—A Review." *Cogent Engineering* 2 (1). https://doi.org/10.1080/23311916.2015.1078018.

[2] Bian, Hui, Kinda Hannawi, Mokhfi Takarli, Laurent Molez, and William Prince. 2016. "Effects of Thermal Damage on Physical Properties and Cracking Behavior of Ultrahigh-Performance Fiber-Reinforced Concrete." *Journal of Materials Science* 51 (22): 10066–76. https://doi.org/10.1007/s10853-016-0233-9.

[3] Deng, Xiao, Wen Yang, Xiao Qin Liu, Bao Jun Cheng, and Tong Liu. 2013. "Study on Properties of Wollastonite Micro Fiber Reinforced Mortar." *Advanced Materials Research* 785–786: 151–56. https://doi.org/10.4028/www.scientific.net/AMR.785-786.151.

[4] DeSouza, S. J., R. D. Hooton, and J. A. Bickley. 1997. "Evaluation of Laboratory Drying Procedures Relevant to Field Conditions for Concrete Sorptivity Measurements." *Cement, Concrete and Aggregates* 19 (2): 59–63. https://doi.org/10.1520/cca10315j.

[5] Dey, V., R. Kachala, A. Bonakdar, and B. Mobasher. 2015. "Mechanical Properties of Micro and Sub-Micron

[6] Wollastonite Fibers in Cementitious Composites." *Construction and Building Materials* 82: 351–59. https://doi.org/10.1016/j.conbuildmat.2015.02.084.
Dey, Vikram, Robert Kachala, Amir Bonakdar, Narayanan Neithalath, and Barzin Mobasher. 2016. "Quantitative 2D
Restrained Shrinkage Cracking of Cement Paste with

[7] Wollastonite Microfibers." *Journal of Materials in Civil Engineering* 28 (9): 1–11. https://doi.org/10.1061/(ASCE)MT.1943-5533.0001592.

[8] Feng, Chi, and Hans Janssen. 2018. "Hygric Properties of Porous Building Materials (III): Impact Factors and Data Processing Methods of the Capillary Absorption Test." *Building and Environment* 134 (January): 21–34. https://doi.org/10.1016/j.buildenv.2018.02.038.

[9] Ghosh, Abhik, V. Sairam, and B. Bhattacharjee. 2013. "Effect of Nano-Silica on Strength and Microstructure of Cement Silica Fume Paste, Mortar and Concrete." *Indian Concrete Journal* 87 (6): 11–25.

[10] Hall, C. 1989. "Water Sorptivity of Mortars and Concretes: A Review.Pdf."

[11] Hall, Christopher, and Andrea Hamilton. 2018. "Beyond the Sorptivity: Definition, Measurement, and Properties of the Secondary Sorptivity." *Journal of Materials in Civil Engineering* 30 (4): 04018049. https://doi.org/10.1061/(asce)mt.1943-5533.0002226.

[12] Hall, Christopher, and William D Hoff. n.d. *Christopher Hall, William D. Hoff - Water Transport in Brick, Stone and Concrete-CRC Press (2002)*.

[13] Hanumanthu, Korakuti, and Kaustav Sarkar. 2021. "Improved Sorptivity Models for Mortar and Concrete Based on Significant Process Parameters." *Journal of Building Engineering* 47 (December 2021): 103912. https://doi.org/10.1016/j.jobe.2021.103912.

[14] Hou, Peng Kun, Shiho Kawashima, Ke Jin Wang, David J. Corr, Jue Shi Qian, and Surendra P. Shah. 2013. "Effects of Colloidal Nanosilica on Rheological and Mechanical Properties of Fly Ash-Cement Mortar." *Cement and Concrete Composites* 35 (1): 12–22. https://doi.org/10.1016/j.cemconcomp.2012.08.027.

[15] J, Kovacik. 2000. "Correlation between Young's Modulus and Porosity in Porous Materials." *Journal of Materials Science Letters* 18 (1–4): 1007–10. https://doi.org/10.1023/A.

[16] Jo, Byung Wan, Chang Hyun Kim, and Jae Hoon Lim. 2007. "Characteristics of Cement Mortar with Nano-SiO 2 Particles." *ACI Materials Journal* 104 (4): 404–7. https://doi.org/10.14359/18830.

[17] Kondraivendhan, B., and B. Bhattacharjee. 2010. "Effect of Age and Water-Cement Ratio on Size and Dispersion of Pores in Ordinary Portland Cement Paste." *ACI Materials Journal* 107 (2): 147–54. https://doi.org/10.14359/51663578.

[18] Kwon, Sukmin, Tomoya Nishiwaki, Heesup Choi, and Hirozo Mihashi. 2015. "Effect of Wollastonite Microfiber on Ultra-High-Performance Fiber-Reinforced Cement-Based Composites Based on Application of Multi-Scale Fiber-Reinforcement System." *Journal of Advanced Concrete Technology* 13 (7): 332–44. https://doi.org/10.3151/jact.13.332.

[19] Levasil, CB. n.d. "Strong Constructions That Last Saving Resources by Improving Performance."

[20] Li, Zongjin, and Zhu Ding. 2003. "Property Improvement of Portland Cement by Incorporating with Metakaolin and Slag." *Cement and Concrete Research* 33 (4): 579–84. https://doi.org/10.1016/S0008-8846(02)01025-6.

[21] Mathur, Renu, A. K. Misra, Pankaj Goel, Renu Mathur, A. K. Misra, and Pankaj Goel. 2007. "Influence of Wollastonite on Mechanical Properties of Concrete." *Journal of Scientific and Industrial Research* 66 (12): 1029–34.

[22] Monteiro, P. J.M., A. P. Kirchheim, S. Chae, P. Fischer, A. A. MacDowell, E. Schaible, and H. R. Wenk. 2009. "Characterizing the Nano and Micro Structure of Concrete to Improve Its Durability." *Cement and Concrete Composites* 31 (8): 577–84. https://doi.org/10.1016/j.cemconcomp.2008.12.007.

[23] Nair, Nishant A., and V. Sairam. 2021. "Research Initiatives on the Influence of Wollastonite in Cement-Based Construction Material-A Review." *Journal of Cleaner Production* 283: 124665. https://doi.org/10.1016/j.jclepro.2020.124665.

[24] Naji Givi, Alireza, Suraya Abdul Rashid, Farah Nora A. Aziz, and Mohamad Amran Mohd Salleh. 2010. "Experimental Investigation of the Size Effects of SiO2 Nano-Particles on the Mechanical Properties of Binary Blended Concrete." *Composites*

[25] *Part B: Engineering* 41 (8): 673–77. https://doi.org/10.1016/j.compositesb.2010.08.003.

[26] Qing, Ye, Zhang Zenan, Kong Deyu, and Chen Rongshen. 2007. "Influence of Nano-SiO2 Addition on Properties of Hardened Cement Paste as Compared with Silica Fume." *Construction and Building Materials* 21 (3): 539–45. https://doi.org/10.1016/j.conbuildmat.2005.09.001.

[27] Ransinchung, G. D., and Brind Kumar. 2010. "Investigations on Pastes and Mortars of Ordinary Portland Cement Admixed with Wollastonite and Microsilica." *Journal of Materials in Civil Engineering* 22 (4): 305–13. https://doi.org/10.1061/(ASCE)MT.1943-5533.0000019.

[28] Ransinchung, G D, Brind Kumar, and Veerendra Kumar. 2009. "Assessment of Water Absorption and Chloride Ion Penetration of Pavement Quality Concrete Admixed with Wollastonite and Microsilica." *Construction and Building Materials* 23 (2): 1168–77. https://doi.org/10.1016/j.conbuildmat.2008.06.011.

[29] Rao, G. Appa. 2003. "Investigations on the Performance of Silica Fume-Incorporated Cement Pastes and Mortars." *Cement and Concrete Research* 33 (11): 1765–70. https://doi.org/10.1016/S0008-8846(03)00171-6.

[30] scrivener, K., R. Snellings, and B. Lothenbach. 2016. *A Practical Guide to Microstructural Analysis of Cementitious Materials*. Edited by K. Scrivener, R. Snellings, and B. Lothenbach. *Taylor & Francis Group*. First. Vol. 1. Boca Raton, FL: CRC Press. https://www.routledge.com/A-Practical-Guide-to-Microstructural-Analysis-of-Cementitious-Materials/Scrivener-Snellings-Lothenbach/p/book/9781138747234.

[31] Scrivener, Karen L, and Alain Capmas. 2004. *Lea's Chemistry of Cement and Concrete. Science*. Vol. 58. http://www.dbpia.co.kr/view/ar_view.asp?arid=1536305.

[32] Sharma, Shashi Kant. 2019. "Properties of SCC Containing Pozzolans, Wollastonite Micro Fiber, and Recycled Aggregates." *Heliyon* 5 (8): e02081. https://doi.org/10.1016/j.heliyon.2019.e02081.

[33] Sharma, U., L. P. Singh, D. Ali, and C. S. Poon. 2019. "Effect of Particle Size of Silica Nanoparticles on Hydration Reactivity and Microstructure of C-S-H Gel." *Advances in Civil Engineering Materials* 8 (3): 346–60. https://doi.org/10.1520/ACEM20190007.

[34] Soliman, A. M., and M. L. Nehdi. 2012. "Effect of Natural Wollastonite Microfibers on Early-Age Behavior of UHPC." *Journal of Materials in Civil Engineering* 24 (7): 816–24. https://doi.org/10.1061/(ASCE)MT.1943-5533.0000473.

[35] Svensson, Kristoff, Andreas Neumann, Flora Feitosa Menezes, Christof Lempp, and Herbert Pöllmann. 2018. "The Conversion of Wollastonite to CaCO3 Considering Its Use for CCS Application as Cementitious Material." *Applied Sciences (Switzerland)* 8 (2). https://doi.org/10.3390/app8020304.

[36] Trezza, M. A., and A. E. Lavat. 2001. "Analysis of the System 3CaO·Al2O3-CaSO4· 2H2O-CaCO3-H2O by FT-IR Spectroscopy." *Cement and Concrete Research* 31 (6): 869–72. https://doi.org/10.1016/S0008-8846(01)00502-6.

[37] Uzoegbo, H. C. 2019. *Dry-Stack and Compressed Stabilized Earth-Block Construction. Nonconventional and Vernacular Construction Materials: Characterisation, Properties and Applications*. Elsevier Ltd. https://doi.org/10.1016/B978-0-08-102

[38] Yang, Lin, Danying Gao, Yunsheng Zhang, Jiyu Tang, and Ying Li. 2019. "Relationship between Sorptivity and Capillary Coefficient for Water Absorption of Cement-Based Materials: Theory Analysis and Experiment." *Royal Society Open Science* 6 (6). https://doi.org/10.1098/rsos.190112.

[39] Zareei, Seyed Alireza, Farshad Ameri, Parham Shoaei, and Nasrollah Bahrami. 2019. "Recycled Ceramic Waste High Strength Concrete Containing Wollastonite Particles and Micro-Silica: A Comprehensive Experimental Study." *Construction and Building Materials* 201: 11–32. https://doi.org/10.1016/j.conbuildmat.2018.12.161.

[40] Zhang, Min Hong, Jahidul Islam, and Sulapha Peethamparan. 2012. "Use of Nano-Silica to Increase Early Strength and Reduce Setting Time of Concretes with High Volumes of Slag." *Cement and Concrete Composites* 34 (5): 650–62. https://doi.org/10.1016/j.cemconcomp.2012.02.005.

****